Journal of Fluorescence (2021) 31:807–815
https://doi.org/10.1007/s10895-021-02711-6

ORIGINAL ARTICLE

Aggregation-induced Emission Properties of Triphenylamine Chalcone Compounds

Ying-Peng Zhang[1] · Qi Teng[1] · Yun-Shang Yang[1] · Jing-Qi Cao[1] · Ji-Jun Xue[2]

Received: 12 January 2021 / Accepted: 3 March 2021 / Published online: 16 March 2021

Abstract

Two triphenylamine chalcone derivatives 1 and 2 were synthesized through the Vilsmeier-Haack reaction and Claisen-Schmidt condensation reaction. Through ultraviolet absorption spectroscopy and fluorescence emission spectroscopy experiments, it was confirmed that these two compounds exhibited good aggregation-induced emission (AIE) behavior in ethanol/water mixtures. The solvent effect test showed with the increase of the orientation polarizability of the solvent, the Stokes shift in the solvent of compound 1 and compound 2 shows a linear change trend. Through solid state fluorescence test and universal density function theory (DFT), the existence of π-π stacking interaction in the solid state of the compound has been studied, resulting in weak fluorescence emission. pH has no effect on the fluorescence intensity of the aggregate state of excited state intramolecular proton transfer (ESIPT) molecules in an acidic environment, but greatly weakens its fluorescence intensity in an alkaline environment. Cyclic voltammetry (CV) test shows that compound 1 was more prone to oxidation reaction than compound 2. The results of thermal stability test show that the thermal stability of compound 1 was better than that of compound 2, indicating that triphenylamine chalcone derivatives can improve the thermal stability of compounds by increasing the number of branches.

Keywords Triphenylamine · Chalcone · AIE · Optoelectronics

Introduction

In recent years, AIE materials have been widely used in chemical sensing, biological imaging, organic light-emitting diodes (OLED) [1–7], etc.Based on a large number of experiments and theoretical studies, researchers have concluded that restriction of intramolecular rotations (RIR), excited state intramolecular proton transfer (ESIPT), etc. [8] inhibits the π-π accumulation in the molecule to achieve the AIE effect. Due to the widespread application of molecules based on the ESIPT mechanism of action [9–11], the behavior of AIE based on the ESIPT mechanism has gradually gained attention in the field of natural sciences. Generally, a molecule with ESIPT characteristics was composed of a proton donor (such as -OH, -NH_2) and a proton acceptor (such as -N = C, C = O) [12]. Because of its π conjugated framework, the fluorescence emission of 2-hydroxychalcone derivatives was often affected by aggregation-caused quenching (ACQ). Triphenylamine was a molecule with a central N atom and three benzene rings connected around it to form a star-shaped structure. Because of its special structure, it has larger steric hindrance and higher hole transport rate [13]. In addition, the structure of triphenylamine was easy to modified. Although the fluorescence emission efficiency of triphenylamine was not high, the modified triphenylamine derivatives were used in fluorescent probes [14–16], organic electroluminescent materials and organic solar cell materials [17, 18] and other aspects have been widely used.

Recently, triphenylamine derivatives have also been extensively studied on AIE behavior [18–24]. Owing to the unique helical structure of triphenylamine, partial access of triphenylamine group to 2-hydroxychalcone can effectively avoid face-to-face π-π accumulation of molecules, inhibit the production of ACQ effects, and enhance its fluorescence in the aggregated state. However, the AIE effect will be affected by different solvents [25–28], different substituents [29–32], pH

✉ Yun-Shang Yang
yangyunshang@tom.comfor

Ying-Peng Zhang
yingpengzhang@126.com

[1] School of Petrochemical Engineering, Lanzhou University of Technology, Lanzhou 730050, China

[2] State Key Laboratory of Applied Organic Chemistry & College of Chemistry and Chemical Engineering, Lanzhou University, 730000 Lanzhou, China

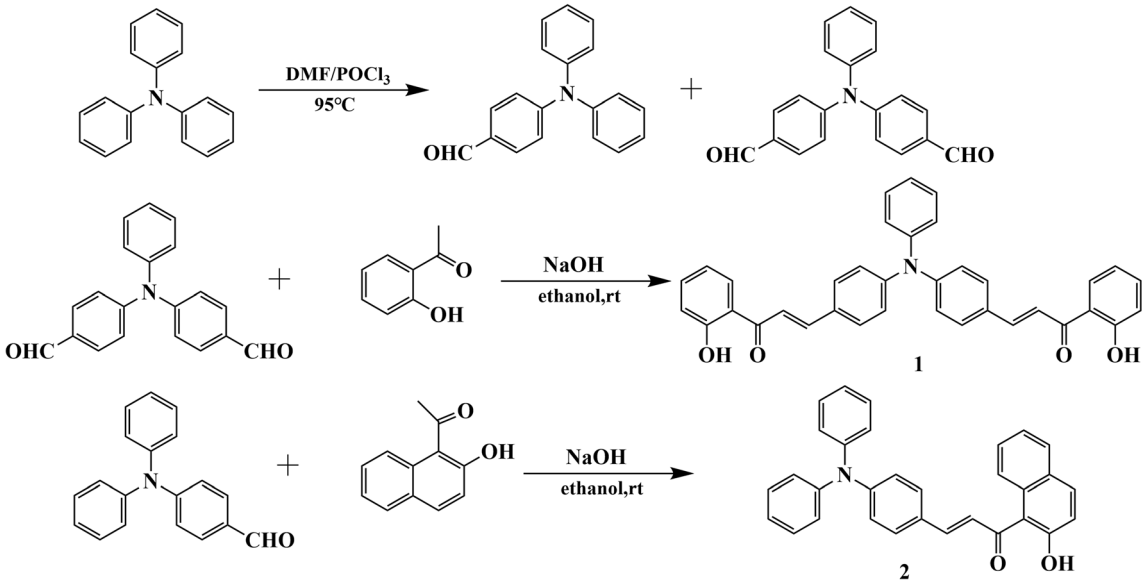

Fig. 1 Synthesis routes of compounds 1 and 2

[33], etc. In view of this, this paper designed and synthesized two triphenylamine chalcone derivatives with different substituents. Because of this, two triphenylamine chalcone derivatives containing different substituents were designed and synthesized, and their AIE behavior was studied in different solvents and ethanol/water mixtures.

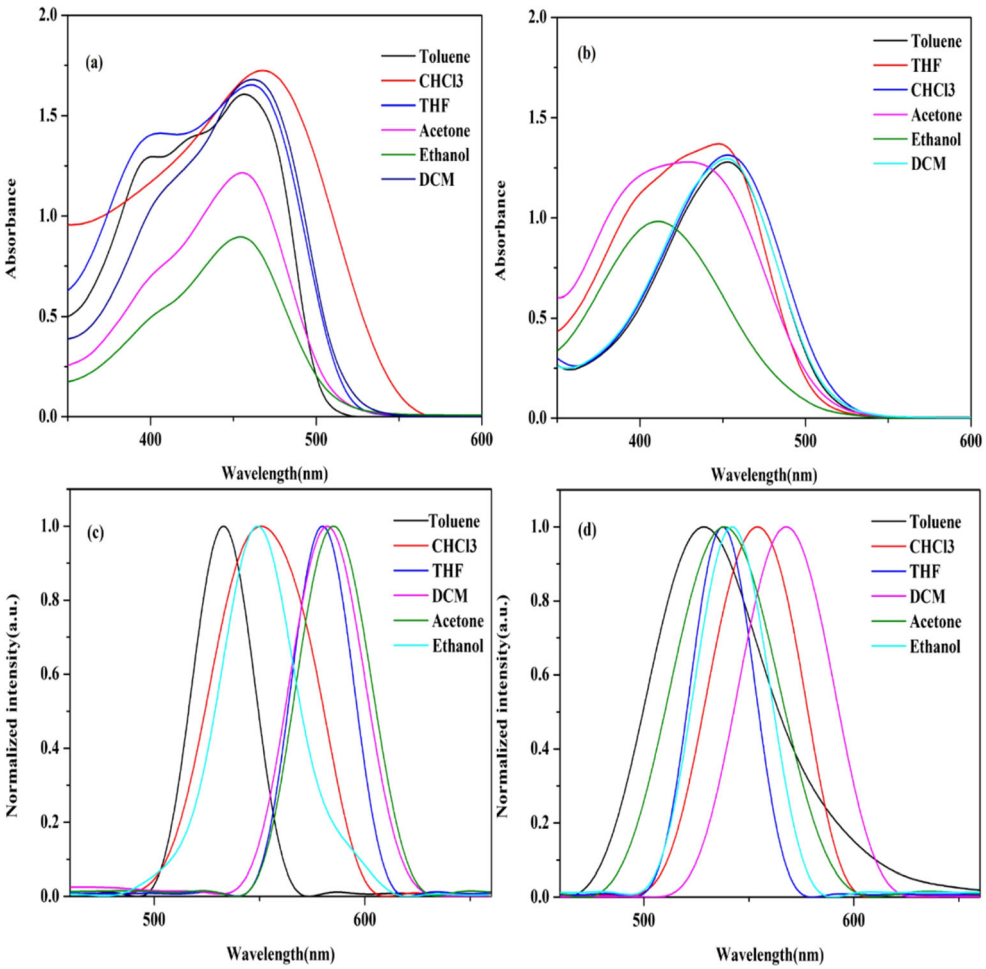

Fig. 2 **a** UV-Vis absorption spectra of compound 1 under different solvents ($c = 1 \times 10^{-5}$ mol/L); **b** UV-Vis absorption spectra of compound 2 under. different solvents ($c = 1 \times 10^{-5}$ mol/L); **c** Normalized fluorescence emission spectra of compound 1 under different solvents ($c = 1 \times 10^{-5}$ mol/L); **d** Normalized fluorescence emission spectra of compound 2 under different solvents ($c = 1 \times 10^{-5}$ mol/L)

Experimental

Materials and Methods

The raw materials required for the experiment such as triphenylamine, phosphorusvoxychloride, N,N-dimethylformamide, 2-hydroxyacetophenone, 2-hydroxy-1-naphthophenone, sodium hydroxide, ethanol, and chloroform. ^{1} H and ^{13} C-NMR spectra were recorded on a Avance 400 spectrometer in $CDCl_3$ with.

TMS as an internal standard. Mass spectrum was recorded on the Thermo Q-Exactive mass spectrometer. The melting point was measured on the XRC-1μ melting point instrument. The ultraviolet absorption was recorded on Cary50. The fluorescence test was recorded on the FE06CN-IF171(ZB) LD/LM luminescence spectrophotometer. Thermogravimetric analysis (TGA) was performed on Mettler STAR^{e} System thermal analyser under nitrogen flushing at a heating rate of 10 min^{-1} with sample weight of 3–4 mg. Cyclic voltammetry measurements were performed on a CHI660E electrochemical workstation at room temperature with three electrodes cell system in a solution of Bu_4NPF_6 (0.1 M) in chloroform at a scanning rate of 100 mVs^{-1}. Glassy carbon electrode acts as working electrode; platinum electrode used as a counter electrode and SCE (saturated calomel electrode) electrode as a reference electrode. The scanning electron microscope images of compound 1 and compound 2 in different ratios of ethanol and water as solvents were tested on Hitachi Regulus 8100 high-resolution cold field emission electron microscope.

Synthesis of Chalcone Compounds

The synthetic route of compound 1 and compound 2 are shown in Fig. 1. 4-Diphenylaminobenzaldehyde and 4,4'-diformyltrianiline were synthesized according to literature [34]. The chalcone compound was synthesized according to literature [35]. 4,4'-dimethylacyl-trianiline (10 mmol) and 2-hydroxyacetophenone (20 mmol) were dissolved in 50 ml anhydrous ethanol, The reaction temperature was controlled below 7 and slowly add 2ml NaOH(21 M) solution to the reaction system. After reaction was stirred for 24 h at 25 , the pure product was obtained by silica gel columnchromatography. M.p.: 191–193 . field 48%, ^{1}H NMR ($CDCl_3$, 400 MHz): δ_H ppm 12.92 (s, 2 H), 7.91 (d, J = 4 Hz, 3 H), 7.87 (s, 1 H), 7.57 (d, J = 2 Hz, 3 H), 7.56 (s, 2 H), 7.54 (s,1 H), 7.48 (t, J = 4 Hz, 2 H), 7.36 (t, J = 4 Hz, 2 H), 7.19 (s, J = 4 Hz, 3 H), 7.14 (s, 2 H), 7.12 (s, 2 H), 7.03 (s, 1 H), 7.01 (s, 1 H), 6.93 (t, J = 4 Hz, 2 H). ^{13} C NMR ($CDCl_3$, 100 MHz): δ_C ppm 193.48, 163.56, 149.38, 146, 144.82, 136.19, 130.09, 129.85, 129.47, 129.10, 126.31, 125.32, 123.31, 120.12, 118.77, 118.60, 118.16. HRMS m/z: calculated for $[M + H]^+$ 538.20, found 538.20144.

5-Diphenylaminobenzaldehyde (10 mmol) and 2-hydroxy-1-naphthaleneethanone (10 mmol) were dissolved in 50ml of absolute ethanol. Then slowly added2ml NaOH (25 M) solution to the reaction system under ice water, reacted ov-ernight at room temperature, and then purified by column chromatography to obtain compound 2. M.p: 191–193 . field: 53 %, ^{1} H NMR ($CDCl_3$, 400 MHz): δ_H ppm 12.60 (s, 1 H), 8.08 (d, J = 4 Hz, 1 H), 7.89 (t, J = 4 Hz, 2 H), 7.79 (d, J = 4 Hz, 1 H), 7.52(t, J = 4 Hz, 1 H), 7.46 (d, J = 4 Hz, 2 H), 7.38 (t, J = 4 Hz, 2 H),7.34 (s, 1 H), 7.30 (t, J = 4 Hz, 4 H), 7.18 (s, 1 H), 7.15 (t, J = 4 Hz, 4 H), 7.11 (t, J = 4 Hz, 2 H), 7.02 (d, J = 2 Hz, 2 H). ^{13} C NMR ($CDCl_3$, 100 MHz): δ_C ppm 194.34, 162.37, 150.39, 146.67, 143.13, 136.33, 131.57, 130.03, 129.54, 129.20, 128.63,127.62, 127.52, 125.61, 125.20, 124.31, 124.22, 123.80,121.29, 119.39, 116.13. HR-MS m/z: calculated for $[M + H]^+$ 442.18, found 442.18012.

Results and Discussion

Solvent Effect

In order to investigate the influence of different solvents on the ESIPT behavior of compound 1 and compound 2, the UV-visible absorption spectrum and fluorescence emission spectrum behavior of compound 1 and compound 2 in acetone, ethanol, dichloromethane, tetrahydrofuran, toluene, and chloroform were studied. It can be seen from Fig. 2(a) and 2(b) that the absorption wavelength maximum was shorter in the protic solvent ethanol. The absorption wavelength was longer in aprotic solvents. As was shown in Fig. 2(c), the maximum emission peak of fluorescence spectrum gradually shifted to long wavelength in toluene, chloroform, tetrahydrofuran, dichloromethane and acetone. In the Fig. 2(d), this change is not observed, which may be caused by different substituents on the triphenylamine group. To understand the effect of solvent polarity on the optical properties of substances, the relationship between the oriented polarizability (Δf) and the corresponding Stokes (Δv

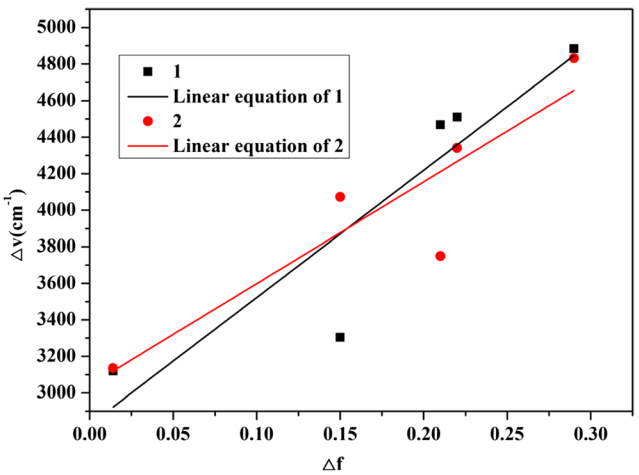

Fig. 3 Lippert mataga plot of compounds 1 and 2 in different solvents

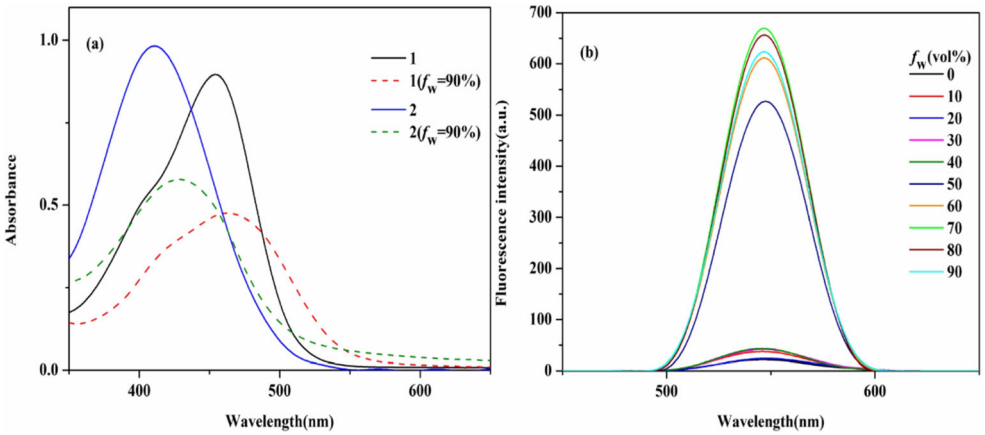

Fig. 4 **a** UV-Vis absorption spectra of compounds 1 and 2 under volume fraction (f_w) of different water in ethanol/water mixtures; **b** Fluorescence emission spectra of compound 1 in ethanol/water mixtures with different volume fractions of water (f_w)

cm^{-1}) of toluene, chloroform, dichloromethane, tetrahydrofuran and ethanol solvents was studied [36]. From Fig. 3 and Table S1, it can be seen that with the increase of the orientation polarizability of the solvent, the Stokes shift in the solvent of compound 1 and compound 2 shows a linear change trend [37].

$$\Delta v = v_{abs} - v_{flu} = \frac{2\Delta\mu^2}{hca^3}\Delta f + \text{constant} \quad (1)$$

$$\Delta f = \frac{\varepsilon - 1}{2\varepsilon + 1} - \frac{\eta^2 - 1}{2\eta^2 + 1} \quad (2)$$

Where, the v_{abs} and v_{flu} are the wavelengths corresponding to the peak of the absorption and emission spectra, respectively. the h was the Planck constant, the c was the speed of light, and the a was the cavity radius. Δμ was the difference between the excited state dipole moment and the ground state dipole moment. ε and η were the dielectric constant and the refractive index of the solvent, respectively.

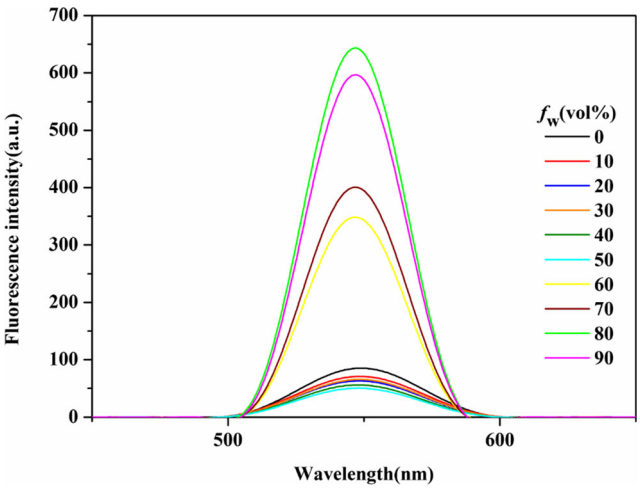

Fig. 5 Fluorescence emission spectra of compound 2 in ethanol/water mixtures with different volume fractions of water (f_w)

AIE Behavior

Chalcone compounds were soluble in ethanol solution and insoluble in water. In order to study whether compound 1 and compound 2 have aggregation-induced emission behavior, the UV absorption spectra and fluorescence emission spectra of chalcone compounds 1 and 2 in different proportions of ethanol/water mixtures were studied. As shown in Fig. 4(a), with the increase of water volume fractions in ethanol/ water mixtures, compounds 1 and 2 show different degrees of decrease of absorption intensity and horizontal trailing phenomenon. The reason for the decrease of absorption intensity may be the light scattering of suspension in aggregate state [38].

Meanwhile, the change of fluorescence intensity caused by the volume content of different water in ethanol/water mixtures was determined at an excitation wavelength of 450nm. As shown in Fig. 4(b), when the volume fraction of water in the ethanol/ water mixtures of Compound 1 was less than 40 %, the fluorescence intensity was not change substantially. When the volume fraction of water was higher than 40 %, the fluorescence intensity gradually increases. As shown in Fig. 5, Compound 2 exhibited similar behavior to compound 1 in ethanol/water mixtures. When

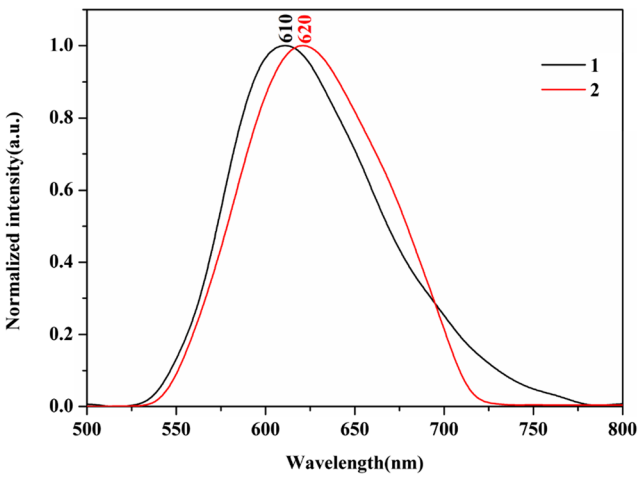

Fig. 6 Normalized solid state fluorescence diagram of compound 1 and 2

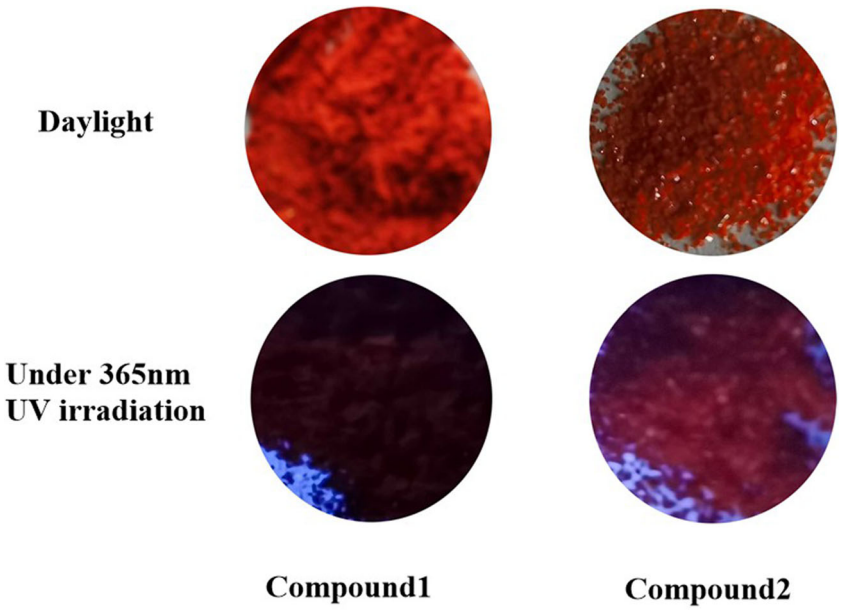

Fig. 7 Photographs of compound1 and compound 2 under daylight and 365nm UV irradiation

the volume fractions of water in ethanol/water mixtures was less than 50 %, the fluorescence intensity was very weak. It may be due to the free rotation of the sigma bond of the benzene ring in the molecule and the distortion of the charge transfer in the molecule, which leads to the destruction of the proton transfer in the excited state [39]. When the volume fractions of water in the ethanol/water mixtures was higher than 50 %, the gradual increase in fluorescence intensity may be due to the carbonyl structure (-C = O) on the chalcone group and the hydroxyl structure (-OH) on the benzene ring undergo an excited state intramolecular proton transfer to form a stable hydrogen bond in aggregate state, which inhibits free rotation within the molecule and enhances fluorescence [40, 41]. Meanwhile, the fluorescence emission behavior of compound 1 and compound 2 in the solid state was also studied. As was shown in Fig. 6, the emission peaks of Compound 1 and Compound 2 in the solid state were 610 nm and 620 nm, respectively. While compounds 1 and 2 had emission peaks of 550 nm and 541 nm in ethanol solvent, respectively. The fluorescence maximum emission peak in the solid state has a red shift of 60nm and 79nm, respectively, relative to the fluorescence maximum emission peak in ethanol solvent. It was caused by the π-π stacking between molecules in the solid state. As was shown in Fig. 7, Under 365nm UV light, the solid state emission of compound 1 was weaker than (E)-3-(4-(diphenylamino)phenyl)-1-(2-hydroxyphenyl)prop-2-en-1-one reported in literature [42]. This phenomenon was

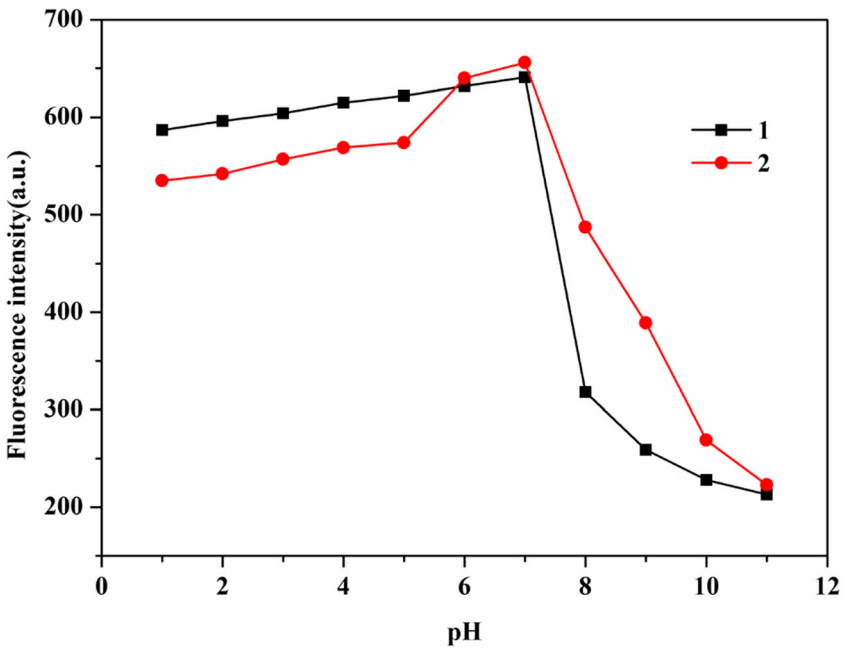

Fig. 8 The fluorescence intensity of compound 1 and compound 2 in ethanol/water mixtures (f_w=90 %) changes with pH

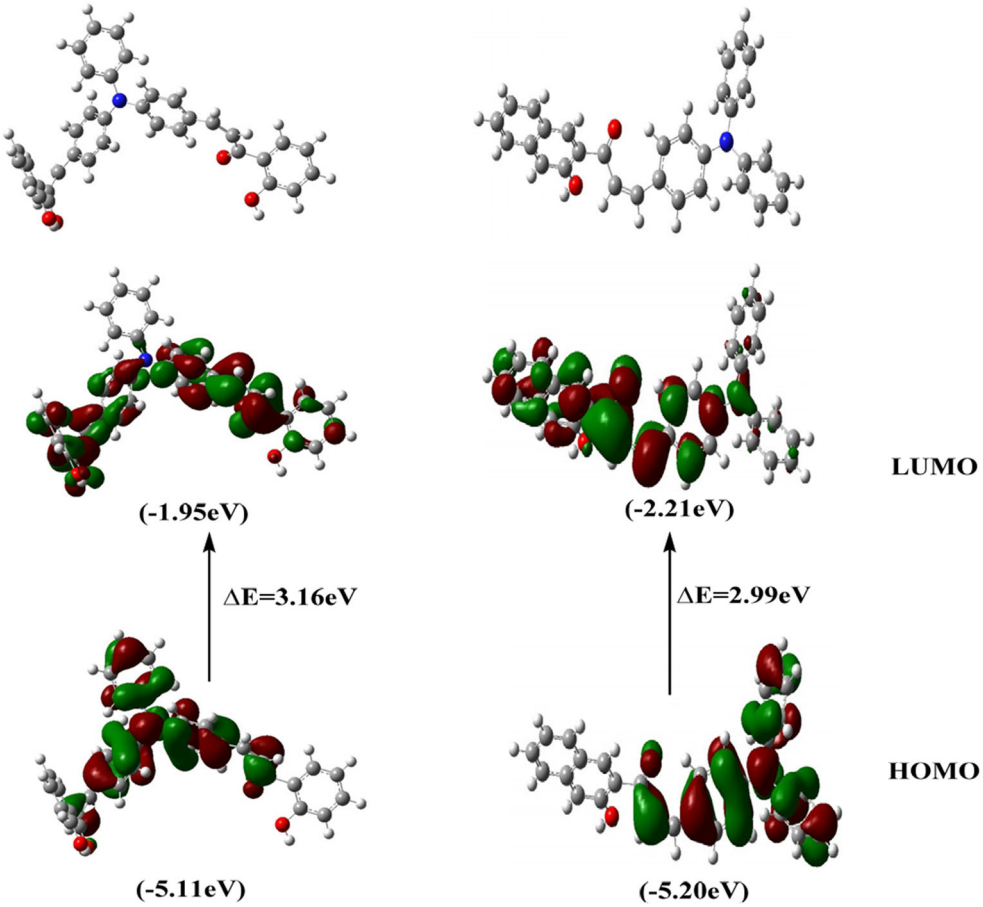

Fig. 9 Optimized structure of compound 1 and compound 2, HOMO and LUMO electron cloud distribution

due to the increase of π-conjugated system, which causes the increase of π-π stacking.

Research on pH Responsiveness

In order to evaluate the effect of pH on the aggregation state of ESIPT molecules, the pH responsiveness of it was studied in an ethanol/water mixtures (f_w=90 %). As was shown in Fig. 8, when the pH was less than 7, compound 1 and compound 2 were maintained in a stable range, without causing much change in fluorescence intensity. It was because the chalcone phenol hydroxyl group was acidic as an acidic proton donor and was insensitive to pH under acidic conditions.When the pH was greater than 7, the fluorescence intensity of compounds 1 and 2 decreased significantly with the increase of pH. It was because the increase of OH^- in the solution

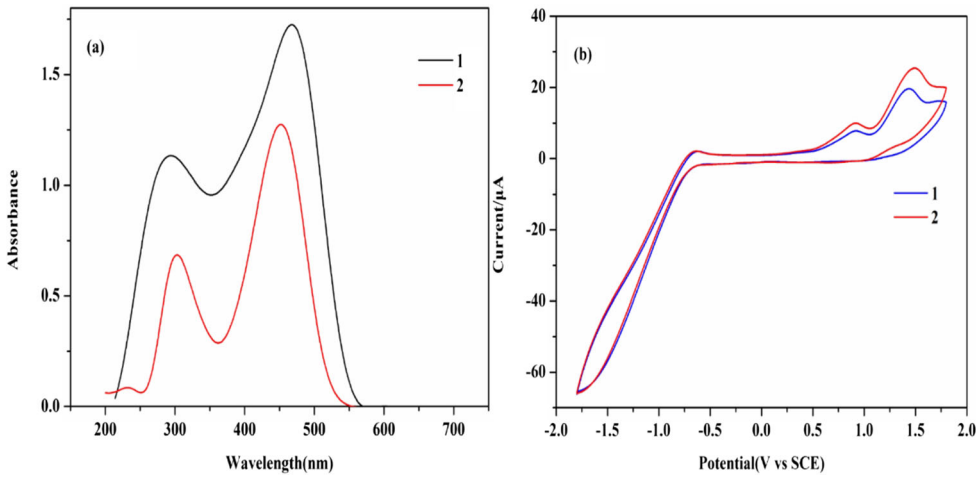

Fig. 10 **a** UV-Vis absorption spectra of compounds 1 and 2 in chloroform solution; **b** Cyclic voltammogram of compound 1 and compound 2 in 0.1 M Bu_4NPF_6-$CHCl_3$

deprives the hydrogen protons on the phenolic hydroxyl group, making it unable to form a stable hydrogen bond, resulting in low fluorescence intensity in the aggregate state.

Theoretical Calculation

In order to have a comprehensive understanding of compound 1 and compound 2 at the molecular level, Gaussian09 software was used to optimize the structure of compounds 1 and 2 with B3LYP/6-31G(d) as the method and basis set. As was shown in Fig. 9, the electron cloud of the highest occupied molecular orbital (HOMO) of compound 1 and compound 2 was mainly distributed in the triphenylamine part, and the electron cloud of the lowest unoccupied molecular orbital (LUMO) was mainly distributed in the corresponding chalcone part. The calculated energy values of the HOMO and LUMO of compound 1 were − 5.11 eV and − 1.95 eV, respectively. The energy values of HOMO and LUMO of compound 2 were − 5.20 eV and − 2.21 eV, respectively. The HOMO-LUMO energy gap (ΔEg) of compound 1 and compound 2 were 3.16 eV and 2.99 eV, respectively. It can be seen from the figure that the optimized spatial configuration of the molecule tends to be planar and fails to effectively prevent π-π stacking, so the fluorescence emission in the solid state was weak.

Electrochemical and Optical Properties

The electrochemical behavior of compound 1 and compound 2 was carried out with $CHCl_3$ as the solvent and tetrabutylammonium hexafluorophosphate as the supporting electrolyte, the electrochemical window is from − 1.8 V to 1.8 V, and the scanning speed was 100mV/s [43]. As was shown in Fig. 10(a), compound 1 and compound 2 were dissolved in chloroform solution, the abscissa of the intersection of the initial line of the absorption wavelength and the long-range absorption spectrum measured by the UV-visible spectrometer was the initial incident wavelength λ_{onset}. Then calculated the energy value of the optical band gap by the formula $E_{opt}=1240/\lambda_{onset}$. The energy values($E_{opt}$) of the optical band gap of compound 1 and compound 2 were 2.24 eV and 2.35 eV, respectively, which may be caused by the different degree of molecular conjugation [44] (Table 1). As was shown in Fig. 10(b), the formation of the oxidation peak may be due to the electron donation of triphenylamine. The initial oxidation potentials of compound 1 and compound 2 were 1.06 V and 1.08 V, respectively.

The initial oxidation potential of compound 1 was slightly lower than that of compound 2, indicating that compound 1 was easier to oxidize than compound 2. Calculated by the formula $E_{HOMO}=-e(E_{onset}^{ox}+4.4)(eV)$, the potentials of the highest occupied molecular orbitals of compound 1 and compound 2 were − 5.46 eV and − 5.48 eV, respectively. The potential of the lowest unoccupied molecular orbital of compound and compound 2 was obtained according to the formula $E_{LUMO}=E_{HOMO}+E_{opt}(eV)$.

Table 1 Electrochemical properties, optical properties

Chalcone Compound	CV		UV	
	HOMO/LUMO (eV)	E_{onset}^{ox} (V)	λ_{onset} (nm)	E_{opt} (eV)
1	-5.46/-3.22	1.06	553	2.24
2	-5.48/-3.13	1.08	528	2.35

Thermal Stability

In order to study the thermal stability of compound 1 and compound 2, the two compounds were tested by thermogravimetric analysis. The 10 % loss of compound mass was defined as the initial value of the thermal decomposition temperature. As was shown in the Fig. 11, the initial thermal decomposition temperature (T_d) of compound 1 and compound 2 were 410 and 340 , respectively. The initial thermal decomposition temperature of compound 1 was higher than that of compound 2, indicating that the derivatives of triphenylamine chalcone can be increased by the number of branches to improve thermal stability. These test results showed that compound 1 and compound 2 have good thermal stability.

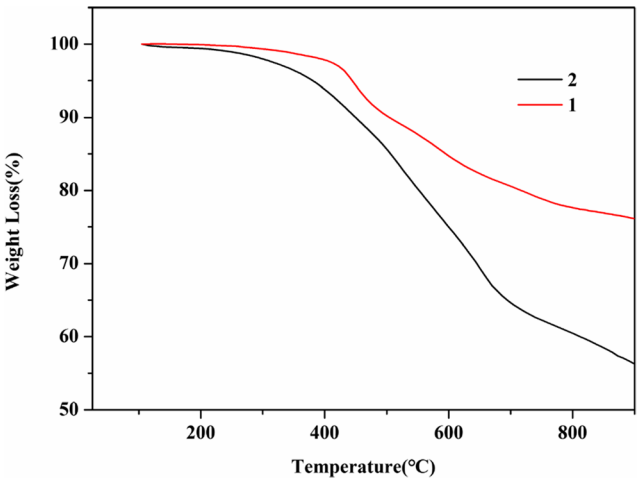

Fig. 11 Thermogravimetric analysis of compound 1 and compound 2

Conclusions

Two triphenylamine chalcone derivatives were synthesized in this chapter, which showed good AIE behavior in ethanol/water mixtures, respectively. The Stokes shift of the solvent shows a linear trend with the increase of the solvent orientation polarizability. Different pH environments will affect the fluorescence intensity of the compound in the aggregate state. Both the solid state fluorescence test and the generalized density function theory show that the two compounds have π-π stacking effect in solid state, which makes the fluorescence emission weak in solid state. Compound 1 is more prone to oxidation than compound 2, and the thermal stability was better than compound 2.

Supplementary Information The online version contains supplementary material available at https://doi.org/10.1007/s10895-021-02711-6.

Author Contributions Ying-Peng Zhang, contributed to the conception of the study;
Qi Teng, performed the experiment and wrote the manuscript;
Yun-Shang Yang, contributed significantly to analysis and manuscript preparation;
Jing-Qi Cao, performed the data analyses;
Ji-Jun Xue, helped perform the analysis with constructive discussions.

Data Availability The ^{1}H NMR, ^{13}C NMR HR-ESI-Ms of the 1 and 2 are detailed in the Supporting information. These materials are available free of charge via the Internet.

Code Availability Not applicable.

Declarations

Conflict of Interest The authors declare that they have no conflict of interest.

References

1. Xie Z, Chen C, Xu S, Li J, Zhang Y, Liu S, Xu J, Chi Z (2015) White-light emission strategy of a single organic compound with aggregation-induced emission and delayed fluorescence properties. Angew Chem Int Ed 127(24):7287–7290
2. Sun J, Lu Y, Wang L, Cheng D, Sun Y, Zeng X (2013) Fluorescence turn-on detection of DNA based on the aggregation-induced emission of conjugated poly (pyridinium salt) s. Polym Chem 4(14):4045–4051
3. Huang J, Jiang Y, Yang J, Tang R, Xie N, Li Q, Li Z (2014) Construction of efficient blue AIE emitters with triphenylamine and TPE moieties for non-doped OLEDs. J Mater Chem C 2(11): 2028–2036
4. Liu M, Zhang X, Yang B, Liu L, Deng F, Zhang X, Wei Y (2014) Polylysine crosslinked AIE dye based fluorescent organic nanoparticles for biological imaging applications. Macromol Biosci 14(9): 1260–1267
5. Jiang R, Cao M, Liu M, Liu L, Huang Q, Huang H, Wei Y (2018) AIE-active self-assemblies from a catalyst-free thiol-yne click reaction and their utilization for biological imaging. Mater Sci Eng C 92:61–68
6. Niu G, Zhang R, Shi X, Park H, Xie S, Kwok RT, Tang BZ (2020) AIE luminogens as fluorescent bioprobes. TrAC Trend Anal Chem 123:115769
7. Mohan M, James J, Satyanarayan MN, Trivedi DR (2019) Functionalized pyrene-based AIEgens: synthesis, photophysical characterization and density functional theory studies. Lumin 34: 715–723
8. Yang W, Li C, Zhang M, Zhou W, Xue R, Liu H, Li Y (2016) Aggregation-induced emission and intermolecular charge transfer effect in triphenylamine fluorophores containing diphenylhydrazone structures. Phys Chem Chem Phys 18(40): 28052–28060
9. Mathivanan M, Tharmalingam B, Lin CH, Pandiyan BV, Thiagarajan V, Murugesapandian B (2020) ESIPT-active multi-color aggregation-induced emission features of triphenylamine–salicylaldehyde-based unsymmetrical azine family. Cryst Eng Comm 22(2):213–228
10. Felouat A, Curtil M, Massue J, Ulrich G (2019) Excited-state intramolecular proton transfer (ESIPT) emitters based on a 2-(2′-hydroxybenzofuranyl) benzoxazole (HBBO) scaffold functionalised with oligo (ethylene glycol)(OEG) chains. New J Chem 43(23):9162–9169
11. Zhou J, Shi R, Liu J, Wang R, Xu Y, Qian X (2015) An ESIPT-based fluorescent probe for sensitive detection of hydrazine in aqueous solution. Org Biomol Chem 13(19):5344–5348
12. Li Y, Ma Y, Yang Y, Shi W, Lan R, Guo Q (2018) Effects of different substituents of methyl 5-R-salicylates on the excited state intramolecular proton transfer process. Chem Chem Phys 20(6): 4208–4215
13. Zhang H, Qu Y, Gao Y, Hua J, Li J, Li B (2013) A red fluorescent 'turn-on'chemosensor for Hg^{2+} based on triphenylamine–triazines derivatives with aggregation-induced emission characteristics. Tetrahedron Lett 54(8):909–912
14. Dumat B, Faurel-Paul E, Fornarelli P, Saettel N, Metgé G, Fiorini-Debuisschert C, Teulade-Fichou MP (2016) Influence of the oxazole ring connection on the fluorescence of oxazoyl-triphenylamine biphotonic DNA probes. Org Biomol Chem 14(1):358–370
15. Li Q, Wang Z, Song W, Ma H, Dong J, Quan YY, Huang ZS (2019) A novel D-π-A triphenylamine-based turn-on colorimetric and ratiometric fluorescence probe for cyanide detection. Dye Pigment 161:389–395
16. Yin J, Peng M, Ma Y, Guo R, Lin W (2018) Rational design of a lipid-droplet-polarity based fluorescent probe for potential cancer diagnosis. Chem Commun 54(85):12093–12096
17. Kong L, Yang J, Zhou H, Li S, Hao F, Zhang Q, Tian Y (2013) Synthesis, photophysical properties and TD-DFT calculation of four two-photon absorbing triphenylamine derivatives. Science China Chem 56(1):106–116
18. Wang Y, Yang C, Li B, Shi F, Gao Y, Wang Z, Peng H (2018) Solvent dependent ultrafast dynamics of multi-branched thiophene-based triphenylamine derivatives with a triazine core. Optik 167: 80–87
19. Yang M, Xu D, Xi W, Wang L, Zheng J, Huang J, Tian Y (2013) Aggregation-induced fluorescence behavior of triphenylamine-based schiff bases: the combined effect of multiple forces. Org Chem 78(20):10344–10359
20. Zhang M, Yang W, Gong T, Zhou W, Xue R (2017) Tunable AIEE fluorescence constructed from a triphenylamine luminogen containing quinoline–application in a reversible and tunable pH sensor. Phys Chem Chem Phys 19(32):21672–21682
21. Usuki T, Shimada M, Yamanoi Y, Ohto T, Tada H, Kasai H, Nishihara H (2018) Aggregation-induced emission enhancement from disilane-bridged donor–acceptor–donor luminogens based

on the triarylamine functionality. ACS Appl Mater Interfaces 10(15):12164–12172
22. Niu G, Zheng X, Zhao Z, Zhang H, Wang J, He X, Tang BZ (2019) AIE-Active Functionalized acrylonitriles with aggregation-induced emission: structure tuning by simple reaction-condition variation, efficient red emission, and two-photon bioimaging. J Am Chem Soc 141(38):15111–15120
23. Wang X, Ding G, Duan Y, Zhu Y, Zhu G, Wang M, Li X, Zhang Y, Qin X, Hung CH (2020) A novel triphenylamine-based bis-Schiff bases fluorophores with AIE-Activity as the hydrazine fluorescence turn-off probes and cell imaging in live cells. Talanta 217:121029
24. Cheng Hr, Ji Y, Liu F, Lu Xj (2019) Rapid and visual detection for hypochlorite of an AIE enhanced fluorescence probe. Lumin 34: 903
25. Satam MA, Telore RD, Sekar N (2014) Photophysical properties of Schiff's bases from 3-(1, 3-benzothiazol-2-yl)-2-hydroxy naphthalene-1-carbaldehyde. Spectrochimica Acta Part a-Molecular Biomolecular Spectroscopy 132:678–686
26. Matsumoto H, Ikedu S, Tosaka T, Nishimura Y, Arai T (2018) Kinetic analysis of tautomer forms of aromatic-urea compounds with acetate ions: solvent effect of excited state intermolecular proton transfer. Photochem Photobiol Sci 17:561–569
27. Chen Y, Yang Y, Zhao Y, Liu S, Li Y (2019) Effect of solvent environment on excited state intramolecular proton transfer in 2-(4-(dimethylamino) phenyl)-3-hydroxy-6,7-dimethoxy-4 h-chromen-4-one. PhysChem Chem Phys 21(32):17711–17719
28. Qi Y, Lu M, Wang Y, Tang Z, Gao Z, Tian J, Liu J (2019) A theoretical study of the ESIPT mechanism of 3-hydroxyflavone derivatives: solvation effect and the importance of TICT for its dual fluorescence properties. Org Chem Front 6(17):3136–3143
29. Ding S, Xu A, Sun A, Xia Y, Liu Y (2021) Substituent effect on ESIPT and hydrogen bond mechanism of N-(8-Quinolyl) salicylaldimine: A detailed theoretical exploration. Spectrochim Acta Part A Mol Biomol Spectrosc 245:118937
30. Ni M, Su S, Fang H (2020) Substituent control of photophysical properties for excited-state intramolecular proton transfer (ESIPT) of o-LHBDI derivatives: a TD-DFT investigation. J Mol Model 26(5):1–10
31. Chrayteh A, Ewels C, Jacquemin D (2020) Dual fluorescence in strap ESIPT systems: a theoretical study. Phys Chem Chem Phys 22(2):854–863
32. Zhang N, Liu G, Yan J, Zhang T, Liu X (2020) Naked diazaborepin dyes: Synthesis, photophysical properties, substituent effects and theoretical calculations on ESIPT process. Dye Pigment 175: 108218
33. Yan L, Qing T, Li R, Wang Z, Qi Z (2016) Synthesis and optical properties of aggregation-induced emission (AIE) molecules based on the ESIPT mechanism as pH- and Zn^{2+}-responsive fluorescent sensors. RSC Adv 6(68):63874
34. Zhu H, Huang J, Kong L, Tian Y, Yang J (2018) Branched triphenylamine luminophores: aggregation-induced fluorescence emission, and tunable near-infrared solid-state fluorescence characteristics via external mechanical stimuli. Dye Pigment 151:140–148
35. Jin H, Li X, Tan T, Wang S, Xiao Y, Tian J (2014) Electrochromic properties of novel chalcones containing triphenylamine moiety. Dye Pigment 106:154–160
36. Bozkurt E, Gul HI, Mete E (2018) Solvent and substituent effect on the photophysical properties of pyrazoline derivatives: A spectroscopic study. J Photochem Photobiol A chem 352:35–42
37. Satam MA, Telore RD, Tathe AB, Gupta VD, Sekar N (2014) A combined theoretical and experimental investigation on the solvatochromism of ESIPT3-(1, 3-benzothiazol-2-yl)-2-hydroxynaphthalene-1-carbaldehyde. Spectrochim Acta Part A Mol Biomol Spectrosc 127:16–24
38. Feng Q, Li Y, Li K, Lu J, Wang J, Fan P, Hou H (2017) Fluorescent chemosensor for zinc ion detection with significant emission color change in aqueous solution based on AIEgen. ChemistrySelect 2(10):3158–3162
39. Fang H, Wang N, Xie L, Huang P, Deng KY, Wu FY (2019) An excited-state intramolecular proton transfer (ESIPT)-based aggregation-induced emission active probe and its Cu (II) complex for fluorescence detection of cysteine. Sens Actuator B-Chem 294: 69–77
40. Liang C, Jiang S (2017) Fluorescence light-up detection of cyanide in water based on cyclization reaction followed by ESIPT and AIEE. Analyst 142(24):4825–4833
41. Sharma S, Virk TS, Pradeep CP, Dhir A (2017) ESIPT-induced carbazole-based AIEE material for nanomolar detection of Cu^{2+} and CN^{-} Ions: a molecular keypad security device. Eur J Inorg Chem 18:2457–2463
42. Li R, Yan L, Wang Z, Qi Z (2017) An aggregation-induced emissive NIR luminescent based on ESIPT and TICT mechanisms and its application to the detection of Cys. J Mol Struct 1136:1–6
43. Chen G, Wang HY, Liu Y, Xu XP, Ji SJ (2010) The synthesis and characterisation of novel pyrazoline derivatives containing triphenylamine. Dye Pigment 85(3):194–200
44. Revoju S, Biswas S, Eliasson B, Sharma GD (2018) Asymmetric triphenylamine–phenothiazine based small molecules with varying terminal acceptors for solution processed bulk-heterojunction organic solar cells. Phys Chem Chem Phys 20(9):6390–6400